# Ultrafast Light-Induced Spin-State Trapping Photophysics Investigated in Fe(phen)₂(NCS)₂ Spin-Crossover Crystal

*Published as part of the Accounts of Chemical Research special issue "Ultrafast Excited-State Processes in Inorganic Systems".*

Roman Bertoni,[†,⊥] Marco Cammarata,[†] Maciej Lorenc,[†] Samir F. Matar,[‡] Jean-François Létard,[‡] Henrik T. Lemke,[§] and Eric Collet*,[†]

[†]Institut de Physique de Rennes, UMR CNRS 6251 Université Rennes 1, Rennes 35042 cedex, France
[‡]ICMCB, CNRS, Université de Bordeaux, 87 avenue du Dr. A. Schweitzer, Pessac 33608, France
[§]LCLS, SLAC National Laboratory, Menlo Park, California 94025, United States

**CONSPECTUS:** Few photoactive molecules undergo a complete transformation of physical properties (magnetism, optical absorption, etc.) when irradiated with light. Such phenomena can happen on the time scale of fundamental atomic motions leading to an entirely new state within less than 1 ps following light absorption. Spin crossover (SCO) molecules are prototype systems having the ability to switch between low spin (LS) and high spin (HS) molecular states both at thermal equilibrium and after light irradiation. In the case of Fe$^{II}$ (3d$^6$) complexes in a nearly octahedral ligand field, the two possible electronic distributions among the 3d split orbitals are $S = 0$ for the LS diamagnetic state and $S = 2$ for the HS paramagnetic state. In crystals, such photoexcited states can be long-lived at low temperature, as is the case for the photoinduced HS state of the [Fe(phen)₂(NCS)₂] SCO compound investigated here.



We first show how such bistability between the diamagnetic and paramagnetic states can be characterized at thermal equilibrium or after light irradiation at low temperature. Complementary techniques provide invaluable insights into relationships between changes of electronic states and structural reorganization. But the development of such light-active materials requires the understanding of the basic mechanism following light excitation of molecules, responsible for trapping them into new electronic and structural states. We therefore discuss how we can observe a photomagnetic molecule during switching and catch on the fly electronic and structural molecular changes with ultrafast X-ray and optical absorption spectroscopies.

In addition, there is a long debate regarding the mechanism behind the efficiency of such a light-induced process. Recent theoretical works suggest that such speed and efficiency are possible thanks to the instantaneous coupling with the phonons of the final state. We discuss here the first experimental proof of that statement as we observe the instantaneous activation of one key phonon mode precluding any recurrence towards the initial state. Our studies show that the structural molecular reorganization trapping the photoinduced electronic state occurs in two sequential steps: the molecule elongates first (within 170 femtosecond) and bends afterwards. This dynamics is caught via the coherent vibrational energy transfer of the two main structural modes. We discuss the transformation pathway connecting the initial photoexcited state to the final state, which involves several key reaction coordinates. These results show the need to replace the classical single coordinate picture employed so far with a more complex multidimensional energy surface.
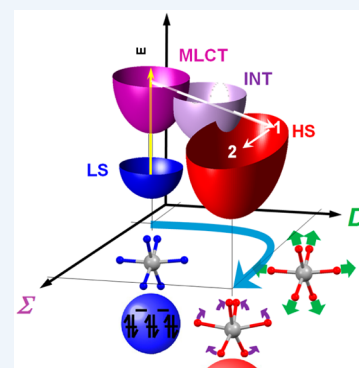
## 1. INTRODUCTION

The response of matter to light on ultrafast (i.e., picosecond and femtosecond) time scales represents a relatively new area in Materials Science. Electronic or structural changes are at the origin of light-activated functions in molecular,[1] biophysical,[2] or solid[3] materials. The past two decades saw remarkable technological advances in ultrafast laser systems and ultrafast science, making it possible to watch the dynamics and to understand the mechanisms of light-induced transformations.

Spin crossover (SCO) molecules[4] are of particular interest because of their ability to switch between low spin (LS) and high spin (HS) molecular states not only under light excitation but also at thermal equilibrium. In the case of Fe$^{II}$ (3d$^6$)

complexes, such as [Fe(phen)₂(NCS)₂] investigated here, two possible electronic distributions among the 3d split orbitals in a nearly octahedral ligand field correspond to the LS ($S = 0$) or HS ($S = 2$) states (Figure 1). The switching from LS to HS after light irradiation is referred to as the light induced excited-spin state trapping phenomenon (LIESST). It was thoroughly investigated in crystals, under continuous light irradiation at low temperature where a complete photoconversion can be easily reached[5−8] or after pulsed irradiation at high temperature.[9−11] Light-induced SCO dynamics was also studied for
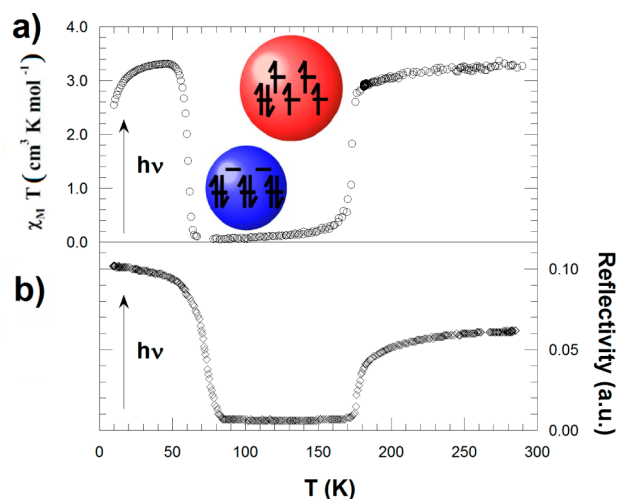
**Figure 1.** (a) Thermal evolution of the $\chi_m T$ product of [Fe-(phen)$_2$(NCS)$_2$] showing a change of spin state around 180 K. The value above 180 K ($\chi_m T \approx 3.3$ cm$^3$·K·mol$^{-1}$) is typical of paramagnetic Fe$^{II}$ HS state, whereas the very small value below 180 K is typical of the LS diamagnetic state. Below 60 K, the HS state is reached by cw light excitation of the LS state at 650 nm. (b) Evolution of the diffuse reflectivity signal recorded at 650 nm and generating LIESST below 60 K.

molecules in solution by the groups of McCusker, McGarvey, Hendrickson, Chergui, Mathies, Schoenlein. The use of ultrafast optical, X-ray, or Raman spectroscopies gave a comprehensive dynamical description of the changes of electronic states and the structural reorganization.[12−25] Our studies of LIESST in Fe$^{III}$ and Fe$^{II}$ SCO crystals,[26−31] as well as reverse-LIESST,[32] indicated a photoswitching dynamics at the molecular level in nano- or microcrystals[11] similar to solution. After introducing how to investigate LIESST effect, we discuss its dynamics, including the coherent structural response recently revealed in [Fe(phen)$_2$(NCS)$_2$].[33]

## 2. THERMAL AND PHOTOINDUCED SPIN-STATE CONVERSION IN Fe(phen)$_2$(NCS)$_2$

[Fe(phen)$_2$(NCS)$_2$] (phen = 1,10-phenanthroline) is an archetypal bistable Fe$^{II}$ SCO crystal.[6,33−37] The diamagnetic LS state of electronic structure $t_{2g}^6 e_g^0 L^0$ (where L corresponds to the LUMO of the ligand) is the ground state. It is of lower entropy than the paramagnetic HS ($t_{2g}^4 e_g^2 L^0$) state observed at high temperature. This change of magnetic state is well characterized by SQUID experiments (Figure 1a). The value of the $\chi_M T$ product ($\chi_M$ being the molar magnetic susceptibility and $T$ the temperature) approaching 3.3 cm$^3$·K·mol$^{-1}$ is characteristic of the paramagnetic HS ($S = 2$) state above 180 K, while below this temperature it corresponds to the diamagnetic LS ($S = 0$) state. Below 60 K, cw light excitation at 650 nm completely transforms the system to the HS state.[38] The change of electronic state also modifies optical properties (Figure 1b). At 650 nm, the higher absorption (lower reflectivity) in the LS state is due to the metal to ligand charge transfer (MLCT) band of the LS state. The electronic redistribution between the LS and HS states is accompanied by an increase of absorption below 620 nm and above 720 nm.[33]

Density functional theory[39,40] calculations (Figure 2) performed with the Gaussian 09 package[41] show that in the LS state the highest occupied molecular orbital (HOMO) and
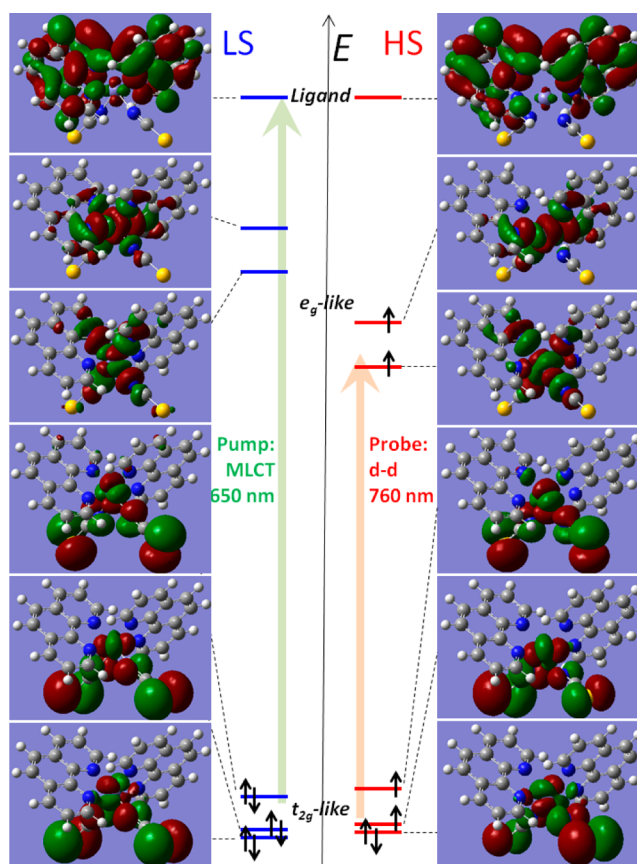


**Figure 2.** Schematic energy diagram and molecular orbitals obtained from DFT calculations. The MLCT process in the LS state with the pump at 650 nm promotes electrons from $t_{2g}$-like to ligand orbitals (L), whereas the probe at 760 nm corresponds to HS $t_{2g}$-like to $e_g$-like d−d transition. The Fe atom is in the center, N atoms are blue, C atoms are gray, S atoms are yellow, and H atoms are white.

lowest unoccupied molecular orbital (LUMO) on both sides of the energy gap are, respectively, of $t_{2g}$- and $e_g$-like character. The $t_{2g}$−$e_g$ energy gap is around 1.8 eV in the LS state and 1.6 eV (775 nm) in the HS state. The LUMO lying ∼1.9 eV above the $t_{2g}$-like LS HOMO has electron density on the ligand phenanthroline groups only. The LS excitation at 650 nm corresponds then to a MLCT (green arrow in Figure 2).

X-ray diffraction reveals important changes of the molecular structure between LS and HS states. The molecule and the Fe atom are located on a 2-fold symmetry axis (Figure 3) of the *Pbcn* (orthorhombic) space group.[6,33] The Fe atom is bonded to N atoms of the two NCS groups and four N atoms of the two phenanthroline groups. The main structural deformations shown in Figure 3 around the FeN$_6$ octahedron are (1) the average Fe−N distance, $\langle$Fe−N$\rangle = (1/6)\sum_{i=1}^{6}$Fe−N$_i$ changes from $\langle$Fe−N$\rangle_{LS} \approx 1.97$ Å to $\langle$Fe−N$\rangle_{HS} \approx 2.16$ Å and (2) the distortion, $\Sigma$ of the FeN$_6$ octahedron, determined by the sum of the deviation from 90° of the 12 N−Fe−N cis $\phi$ angles in the coordination sphere, $\Sigma = \sum_{i=1}^{12}|90 - \phi_i|$ changes from $\Sigma_{LS} \approx 35°$ to $\Sigma_{HS} \approx 65°$.

These structural parameters (Figure 3b) are related to the spin state, and the photoinduced state generated at low temperature is very similar to the HS one.[4,13,15,20−22,24] The $\langle$Fe−N$\rangle$ elongation in the HS state is associated with the electronic population of less bonding $e_g$ orbitals. The increase of $\Sigma$, due to N−Fe−N bending, was underlined as essential for
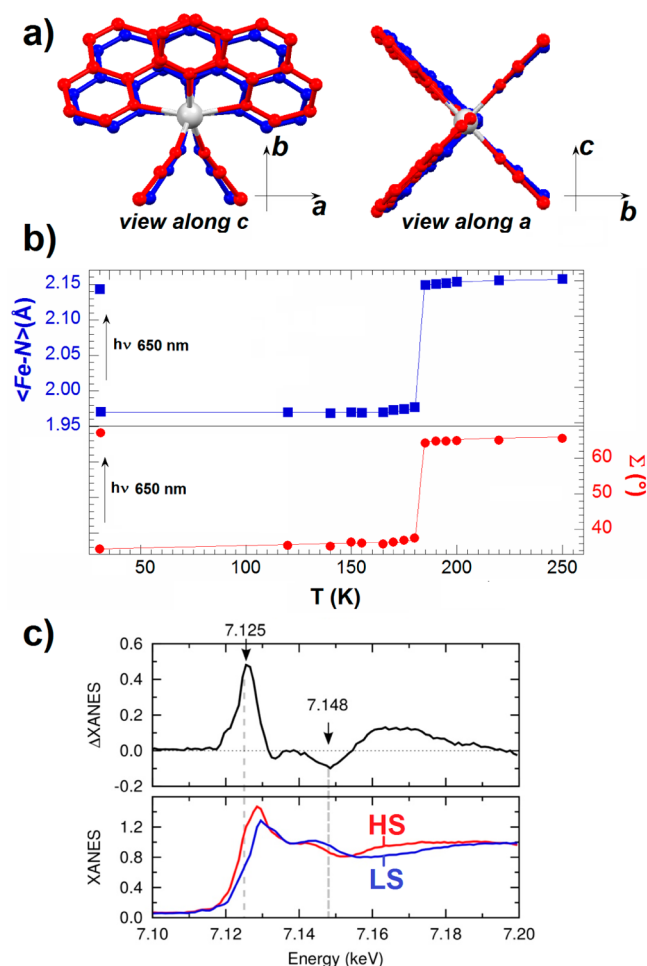
**Figure 3.** (a) LS (140 K, blue) and HS (200 K, red) structures of $[Fe(phen)_2(NCS)_2]$. (b) Temperature dependence of Fe−N bonds and $\Sigma$ parameter, showing the first-order phase transition around 180 K between LS and HS states. The parameters obtained after cw irradiation at 650 nm are identical to those of the HS state at high temperature. (c) XANES spectra and variation $\Delta$XANES measured between the HS (200 K) and LS (140 K) states. Adapted with permission from ref 33. Copyright 2014 American Physical Society.

stabilizing the photoinduced HS state at higher $T$(LIESST).[6] Consequently, the equilibrium position in the HS potential is moved away from that of LS.[8] This electronic conversion accompanied by deformations of the Fe−N$_6$ octahedron, result in important changes of the XANES (X-ray absorption near edge structure) spectrum around the Fe K-edge (Figure 3c).

Magnetic susceptibility directly probes the HS fraction of the crystal. Unfortunately this technique is too slow for investigating the photoswitching dynamics on the time scale of elementary electronic, atomic, or molecular motions, typically falling in the subpicosecond range. This limitation is overcome by ultrafast optical and X-ray spectroscopies that can now routinely achieve 100 fs time resolution. Here we take advantage of the optical and X-ray fingerprints of electronic and structural changes to investigate the photoswitching dynamics from LS to HS states.

# 3. ULTRAFAST PHOTOPHYSICS IN Fe(phen)$_2$(NCS)$_2$ CRYSTALS

## 3.1. Femtosecond Optical and X-ray Absorption Spectroscopy Studies

We recently reported on the ultrafast spin state photoswitching dynamics studies in $[Fe(phen)_2(NCS)_2]$ performed with two complementary pump−probe techniques: XANES and optical spectroscopy. A ∼50 fs pump laser pulse (650 nm) switches LS state to HS via a metal-to-ligand charge-transfer process (MLCT). The changes in XANES are recorded with ∼30 fs X-ray pulses at the XPP station of the LCLS X-FEL, while changes in optical reflectivity (OR) and transmission (OT) in visible−infrared range are recorded with ∼50 fs pulses. For both experiments, the time resolution was ∼110 fs, and more details can be found in ref 33. The measurements presented hereafter were performed at 140 K in the pure LS state. For optical measurements we used single crystals of losange shape (Figure 4) with $a$ and $b$ crystalline axes as, respectively, smallest
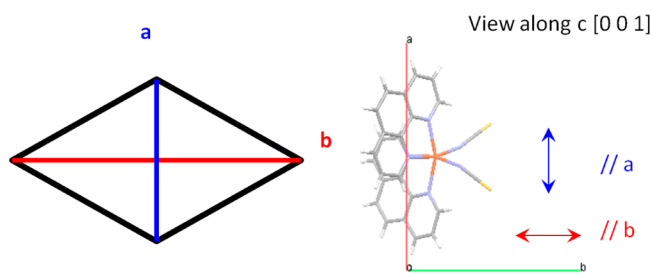


**Figure 4.** Schematic representation of the single crystals of $[Fe(phen)_2(NCS)_2]$ with the orientation of the crystal axes. The 2-fold molecular axis is along the $b$ axis.

and longest diagonals. The 2-fold symmetry axis of the molecule is oriented along the $b$ axis. The $c$ axis corresponds to the crystal thickness. The pump pulse was polarized along the $b$ axis, whereas both polarizations were used for the probe to measure reflectivity. XANES measurements were done on powder films for maximizing X-ray penetration.

The change of molecular structure is monitored by femtosecond XANES around the K edge of iron, which is very sensitive to the change of Fe−N bond length (Figure 3c). Figure 5 shows the time evolution of X-ray absorption at 7125 eV (increase) and 7148 eV (decrease) after excitation, which
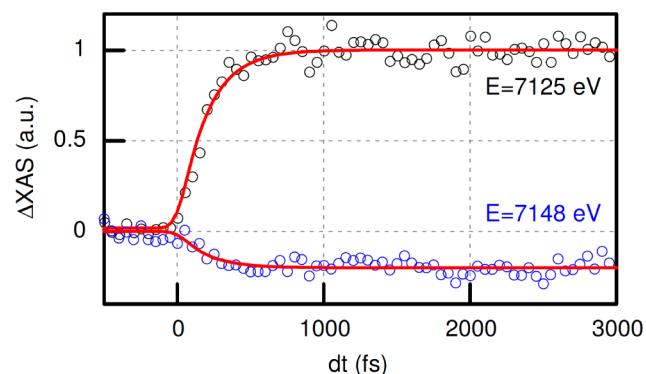


**Figure 5.** Time resolved change of X-ray absorption at 7125 and 7148 eV. Red lines are fit to single exponential rise with time constant $\tau_{\langle Fe-N \rangle} = 170(20)$ fs. Adapted with permission from ref 33. Copyright 2014 American Physical Society.

are the clear fingerprints of the formation of the HS molecular structure. The resulting dynamics can be fit by an exponential rise convoluted with a Gaussian instrument response function.[33] The extracted time constant of $\tau_{\langle Fe-N \rangle}$ = 170(20) fs for the $\langle Fe-N \rangle$ elongation is similar to the time scales reported for other SCO molecules in solution.[20,22]

Figure 6 shows optical changes observed on single crystals, when the probe polarization is parallel to the $b$ axis. At the
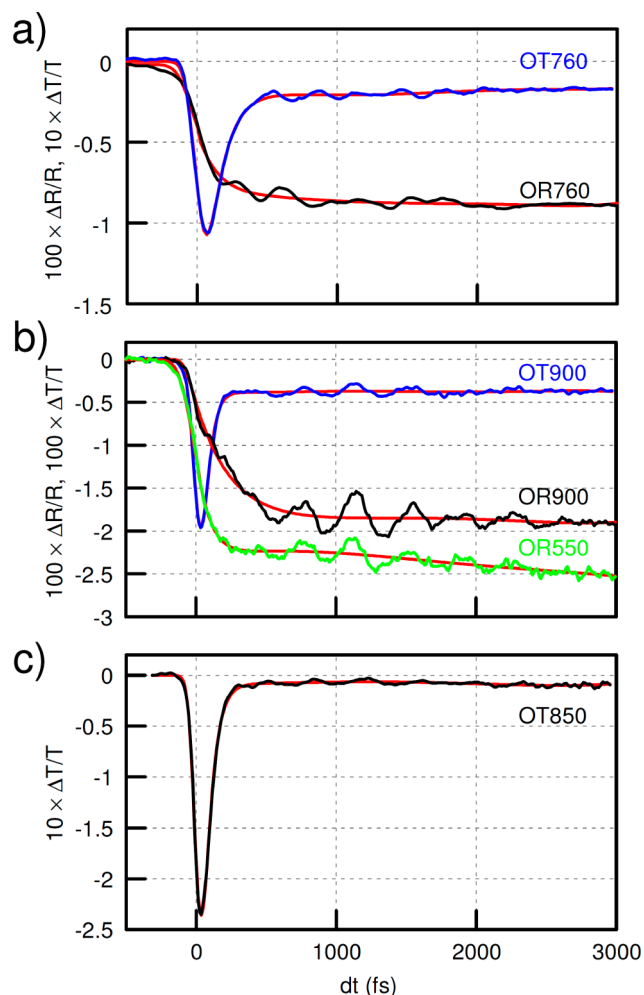


**Figure 6.** Time resolved traces of optical transmission (OT) and reflectivity (OR) at (a) 760 nm, (b) 900 and 550 nm, and (c) 850 nm with probe polarization parallel to $b$ axis. All traces were fitted (red lines) with a single exponential function accounting for the fast dynamic and a fifth order polynomial to take into account slower processes such as vibrational cooling. Adapted with permission from ref 33. Copyright 2014 American Physical Society.

energy of 1.6 eV (760 nm), both transmission and reflectivity show a decreasing signal related to the absorption of the HS state, which corresponds to d−d transitions (see section 3.2). The LS state is optically silent at 760 nm since the lowest $t_{2g}$-like HOMO and $e_g$-like LUMO is at higher energy (Figure 2). The absorption of the HS state at 1.6 eV results therefore from the d−d gap narrowing.[33] Data at 760 nm show that this change occurs within $\tau_{gap}$ = 140(20) fs. Since this ligand field weakening is related to the elongation of the $\langle Fe-N \rangle$ bond length, $\tau_{gap}$ correlates well with $\tau_{\langle Fe-N \rangle}$ = 170(20) fs measured by XANES. Our results demonstrate that by probing a transition sensitive to the ligand field, by means of optical

spectroscopy, it is possible to gain some insight into structural dynamics of the Fe−N$_6$ octahedron. The electronic peak observed at 850 and 900 nm, corresponds to the photoexcited singlet $^1$MLCT state ($t_{2g}^5 e_g^0 L^1$). It decays within less than 50 fs and cannot be well resolved with 100 fs time resolution.[33] Other intermediate (INT) states can be involved in the intersystem crossing (ISC) and the $^{1,3}$MLCT → $^3$T → HS sequence dominates.[42]

The optical kinetic traces shown in Figure 6 also exhibit oscillating components both in reflectivity and in transmission geometries. They are the signatures of molecular vibrations accompanying the LIESST, and similar oscillations were observed first in Fe(bpy)$_3$ by Chergui et al.[19] The oscillating components shown in Figure 7 were extracted from the fit of the data shown in Figure 6.[33] The time-dependent fast Fourier transform trace at 760 nm reveals a main mode at around
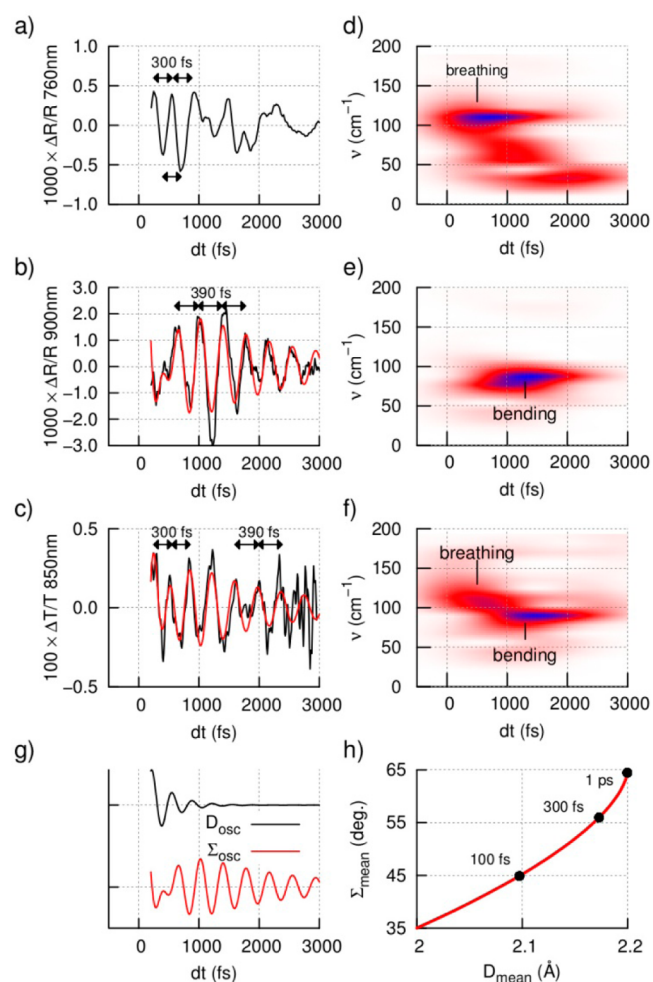


**Figure 7.** (a−c) Oscillating component of OR at 760 nm, OR at 900 nm, and OT at 850 nm. (d−f) Time-dependent FFT of the experimental data, showing the activation of the breathing mode and the delayed activation of the bending mode. Combined fits of OR at 900 nm and OT at 850 nm (red line) by the coupled oscillator model, which show the contribution of the bending ($\Sigma$) mode (b) and the superposition of bending ($\Sigma$) and breathing ($D$) modes (c). The time course of the oscillating component $D_{osc}$ (300 fs) and $\Sigma_{osc}$ (390 fs) obtained by the fit in panels b and c are displayed in panel g, and the average evolutions of $D_{mean}$ and $\Sigma_{mean}$ obtained by the fit in Figure 3 are displayed in panel h. Adapted with permission from ref 33. Copyright 2014 American Physical Society.

113 cm$^{-1}$, which is only observed during the first picosecond. Other reflectivity traces reveal another oscillation around 85 cm$^{-1}$, in-phase for all the probing wavelengths and observed both in transmission and reflectivity.

Different wavelengths are sensitive to different degrees of freedom. The response at 760 nm is, as discussed above, mostly sensitive to the Fe−N core expansion, while the signal at 900 nm is mostly sensitive to the bending of the molecules (this remarkable difference is rationalized by using time-dependent DFT calculations as discussed below). The exponential fits of optical reflectivity at these wavelengths show significantly different time scales thus suggesting a nonsimultaneous expansion and distortion of the molecule as depicted in Figure 7h where the two exponential time constants (from OR 760 nm and OR 900 nm) are used to reconstruct the average evolution of the two structural parameters. To test this hypothesis even further we have modeled a simple coupled oscillator whereby the initial elongation of the Fe−N core induces the octahedral distortion. This model discussed in detail in ref 33 can reproduce fairly well the oscillating part of the experimental data as shown in Figure 7, panels b and c.

To further this investigation, we present in Figure 8 new measurements at 760 nm with probe light polarized parallel or
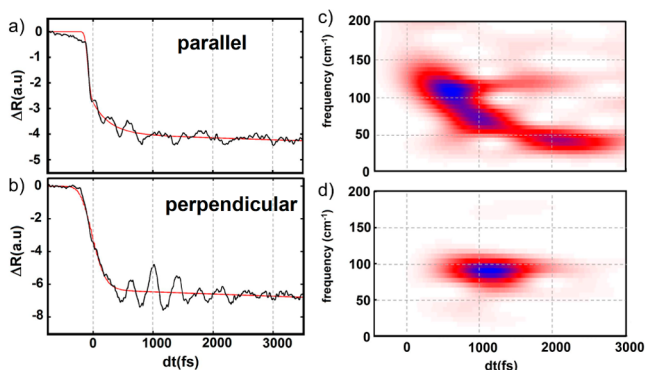


**Figure 9.** (a) Schematic representation of the elongation and damping of the breathing mode along the $D$ coordinate. (b) Classical trajectory in the $(D,\Sigma)$ space. Molecules in the LS (blue) potential reach the $^1$MLCT state by light excitation. Fast ISC, through possible INT states, drives $D$ elongation during step 1 with the generation and damping of the breathing phonon, followed by activation of additional bending phonons, such as distortion $\Sigma$, during step 2. The sequence is sketched at the bottom. Adapted with permission from ref 33. Copyright 2014 American Physical Society.



**Figure 8.** Time resolved change of reflectivity at 760 nm (1.6 eV) for probe polarization parallel (a) or perpendicular (b) to the molecular 2-fold symmetry axis. Red lines are fits obtain with single exponential rise plus a fifth order polynomial. (c, d) Associated TD-FFT showing both breathing and bending depending on the polarization.

perpendicular to the crystal axis $b$, while keeping all other experimental parameters identical. The data for the parallel configuration reproduces well the ones already published in ref 33 (Figure 7), indicating the activation and damping of a mode around 113 cm$^{-1}$ during the first picosecond. However, the data for the polarization perpendicular to $b$, show a different behavior as the frequency of the observed mode is 85 cm$^{-1}$.

### 3.2. Discussion

Recent theoretical studies by van Veenendaal discuss the mechanism behind the extremely fast and efficient ISC during LIESST in terms of dephasing of the photoexcited state into the HS phonon states.[43,44] The change from LS to HS states, which strongly differ in both electronic configuration and molecular structure (metal−ligand distance), is mediated by the spin−orbit coupling. The ultrafast ISC is displacive as the ⟨Fe−N⟩ bond elongation drives the system into the HS potential. Its strong damping is associated with the efficient self-trapping of the photo-induced HS state, as schematically shown in Figure 9a. Our results shown in Figures 6 and 7 strongly support this
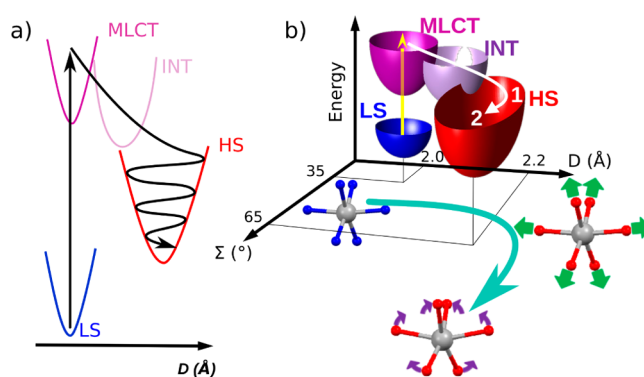
mechanism. The 113 cm$^{-1}$ mode is activated just after light excitation, as Fe−N elongates, and corresponds to the molecular breathing mode: a totally symmetric Fe−N stretching with respect to the 2-fold molecular axis.[33,45,46] This eigenvector of symmetry $A$ in the $C_2$ point group of the complex is hereafter referred to as the breathing coordinate $D$. Figure 6b,c also revealed the activation of a second mode at 85 cm$^{-1}$, corresponding to the butterfly mode,[33,45,46] which bends the ligand and the N−Fe−N angles without significantly changing Fe−N distances. We will refer to this mode as a bending coordinate $\Sigma$. Unlike the breathing mode, activated instantaneously, the bending mode with 390 fs period appears only after 500 fs and has a maximal amplitude around 1200 fs (Figures 7 and 8). Such delayed activation of other modes results from the fact that the HS potential is reached with excess energy. Then the nonequilibrium vibrational energy relaxation in the product HS state activates other modes. Figures 7 and 8 show a spectral weight transfer from breathing to bending. The structural stabilization occurs over two steps with a sequential activation of breathing then bending via coherent energy transfer.

For understanding why the observation of specific vibrational modes depends on the probe energy or polarization, an accurate description of excited states is needed. The time-dependent DFT (TD-DFT) approach has proved an excellent tool used in quantum chemistry.[47] The results obtained within TD-DFT lead to the so-called "natural transition orbitals" (NTOs) through an account for hole−particle pairs, which are then used to interpret the excited states corresponding to the absorption of the probe light. TD-DFT as implemented in the Gaussian 09 package[41] was applied for obtaining the NTOs of HS [Fe(phen)$_2$(NCS)$_2$] starting from a geometry optimized molecule with UB3LYP/6-31g(d,p) functional-basis set. Figure 10a shows the NTO corresponding to the hole−particle transition state around 760 nm for polarization parallel to the $b$ axis. The strong weight of the particle orbital on the Fe−N bonds explains its sensitivity to the breathing mode, for which the Fe−N elongation is the main characteristic. Figure 10b shows the transition state around 760 nm for polarization perpendicular to the $b$ axis; Figure 10c,d shows the transition
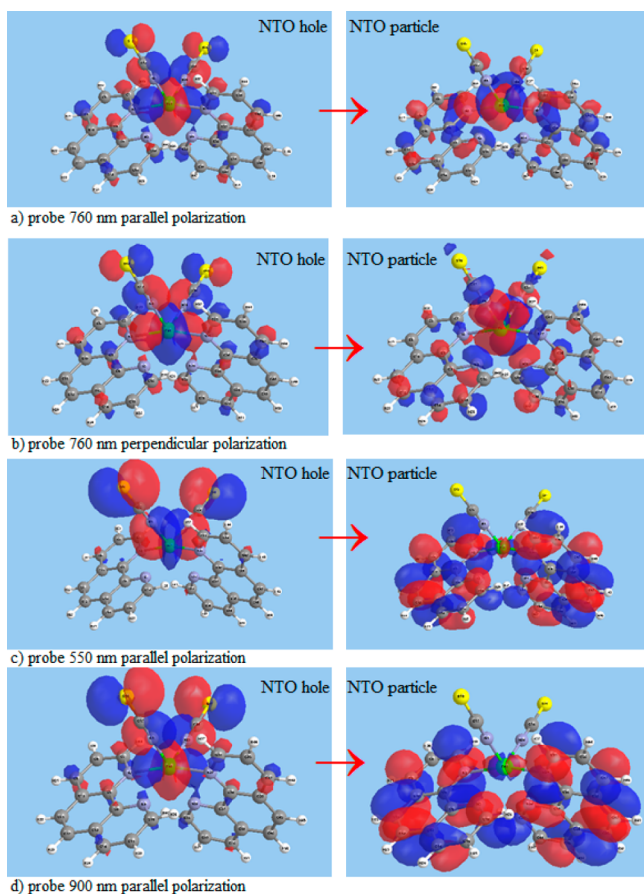
**Figure 10.** NTO of hole and particle for different light polarizations indicated in figure, with respect to the 2-fold molecular symmetry axis, around 760 nm calculated at 1.668 eV (a), around 760 nm calculated at 1.667 eV (b), around 550 nm and calculated at 2.2 eV (c), and around 900 nm calculated at 1.32 eV (d).

state around 550 and 900 nm, respectively, for polarization parallel to the $b$ axis. For these last three cases, the sensitivity to the bending mode observed in Figure 6b is explained by the weight of the particle orbital mainly located on the ligand (not on the Fe−N bonds). This selectivity in terms of light polarization, which can be used in the solid state, opens interesting opportunities for disentangling complex transformation dynamics where different degrees of freedom are involved.

### 3.3. Curved Trajectory on the Potential Energy Surface

We can now summarize all these results in a global picture for describing the photophysics of LIESST. An ultrafast ISC from the MLCT state ($\tau < 50$ fs) occurs, and the less bonding HS potential is rapidly reached, defining a new equilibrium Fe−N bond length. Intermediate states serving as mediators appear in the process but are difficult to identify here. For reaching the minimum of the HS potential, this bond elongation, corresponding to the reaction coordinate $D$, occurs within $\sim$170(20) fs. But as the HS potential is reached with excess kinetic, it has excess kinetic (vibrational) energy; the molecule oscillates along the $D$ coordinate as schematically represented in Figure 9a. The single Fe−N elongation is not enough for stabilizing the HS state, because the minimum of the HS potential corresponds to a distorted structure with different value of $\Sigma$. The delayed activation of the bending mode indicates a two-step process where the coherent dynamics along

$\Sigma$ occurs well after the initial elongation of $D$. The transformation from the initially excited LS state to the trapped HS state can be described on a potential energy surface (PES) where $D$ and $\Sigma$ are the two main reaction coordinates. Figure 9b is a cartoon of such a PES of $[\text{Fe(phen)}_2(\text{NCS})_2]$, where the LS potential has minimum at ($D_{LS} = 1.97$ Å, $\Sigma_{LS} = 35°$) and the one of the HS state at ($D_{HS} = 2.16$ Å, $\Sigma_{HS} = 65°$) (Figure 3b). The analysis of XANES, OT, and OR data[33] gave an average elongation, $D_{mean}(t)$, with a $\sim$170 fs time constant, whereas the average torsion $\Sigma_{mean}(t)$ occurs with a 250 fs time constant (Figure 7h). The system therefore follows a curved trajectory in the $(D,\Sigma)$ coordinate space of the PES, with a sequential activation of the key modes. This process involves a very fast energy transfer: the breathing mode is damped on a time scale of 160 fs (Figure 7g). This strong damping hinders recurrence to the initial state and explains why the structural trapping is so efficient.

### 4. CONCLUSION

This comprehensive study allows drawing an elaborate scenario explaining the speed and efficiency of LIESST, underlying the importance of structural dynamics and energy dissipations. The curved trajectory on the PES, involving coherent structural dynamics, reveals the basic dynamical transformation mechanism associated with a deterministic process.

In order to understand the physical processes allowing functionalization with light, probes sensitive to specific degrees of freedom are mandatory. Ultrafast techniques now allow us to follow and disentangle the dynamical changes of electronic and structural degrees of freedom. Such multiprobe ultrafast studies will become routine in the field of light-functionalized materials, and the present results pave the way for investigating more complex phenomena. Because it is now possible to reach a time resolution better than elementary molecular motions, processes driven by coherent structural dynamics can be deeply investigated. It will represent an important topic in light-activated functions, because this mechanism allows them to reach the shortest time scale for structural trapping, corresponding to the elementary molecular deformations.

### ■ AUTHOR INFORMATION

**Corresponding Author**

*E-mail: eric.collet@univ-rennes1.fr.

**Present Address**

[⊥]R.B.: Fritz Haber Institute of the Max Planck Society, 14195 Berlin, Germany.

**Notes**

The authors declare no competing financial interest.

**Biographies**

**Roman Bertoni** was born in 1987 in France. He received his master degree in Physics from University Rennes 1 in 2010. He obtained his

Ph.D. at the University of Rennes 1 in 2013. He is currently a postdoctoral researcher at the Fritz Haber Institute in Berlin.

**Marco Cammarata** was Born in Palermo, Italy, in 1979. He obtained his Master (2002) and Ph.D. at the Palermo University (2006). He was a Postdoctoral Fellow at the Center for Molecular Movies (2006–2009, University of Copenhagen) and Staff Scientist at SLAC National Laboratory on the X-FEL LCLS (2009-2011, Stanford). Since 2011, he has been a researcher at CNRS. His major research interests concern fast and ultrafast dynamics of molecules in solution (including biomolecules) and photoactive materials.

**Maciej Lorenc** was born in 1974 in Poznan, Poland. He obtained his Ph.D. in 2001 from UAM, Poznan. In 2002, he joined Michael Wulff's group at ESRF in Grenoble and used picosecond X-ray diffraction to study molecular dynamics in solution. In 2005, he joined CNRS and since has held scientist position at the Institute of Physics of Rennes University. In 2013, he received a habilitation degree from Rennes University. His main research interest now is focused on the photoinduced phase transitions.

**Samir F Matar** was born in 1953 in Beirut, Lebanon. He has French (and Lebanese) citizenship. He obtained his degrees at University of Bordeaux, B.Sc., M.Sc., and two Ph.D. He was formerly Assistant Professor at Lebanese University, Professor at Holy Spirit University, and Honorary Dean (Lebanon). Since 1985, he has been a full time researcher at French National Research Center (CNRS) at Institut de Chimie de la Matière Condensée de Bordeaux, ICMCB, Bordeaux-France. His present title is first class research director (DR1-CNRS), Scientific director of the Supercomputer Center of the University of Bordeaux.

**Jean François Létard** was born in 1967 in France and studied Chemistry and Photochemistry at the University of Bordeaux. He received his Ph.D. in 1994 and then obtained an Alexander Von Humboldt fellowship at the University of Mainz (Germany) with the Pr. P. Gütlich. In 1995, he was appointed as CNRS researcher and joined the Molecular Sciences Group of Pr. O. Kahn at the Bordeaux Institute of Condensed Matter Chemistry (ICMCB). His main research interests focus on the elaboration of switchable molecular materials with particular emphasis on photomagnetism and on bistability in connection with industrial applications.

**Henrik T Lemke** was born 1979 in Cologne, Germany. He obtained his Diploma in 2005 (Physics department, University of Kiel, Germany) and his Ph.D. in 2009 (Niels Bohr Institute, University of Copenhagen, Denmark). He worked as a postoctoral researcher for the EU project Organic Nanomaterials for Electronics and Photonics (ONE-P, 2009) before he started to work as an Instrument scientist at the X-FEL Linac Coherent Light Source (LCLS) since 2011 at the SLAC National Laboratory. His research interest deals with non-equilibrium processes in functional materials in liquid and solid state.

**Eric Collet** was born in 1972 in Brittany, France. He obtained a Ph.D. (1999) degree from University of Rennes 1 and was a Postdoctoral Fellow at Laboratoire Léon Brillouin (CEA). In 2007, he became full professor at University Rennes 1. In 2008, he obtained a junior chair at the Institut Universitaire de France. His main topics of interest concern photoinduced phase transitions, their ultrafast structural dynamics, and out-of-equilibrium physics.

## ■ REFERENCES

(1) Zewail, A. H. Femtochemistry: Atomic-scale dynamics of the chemical bond using ultrafast lasers. *Angew. Chem., Int. Ed.* **2000**, *112*, 2586–2631.

(2) Polli, D.; Altoè, P.; Weingart, O.; Spillane, K. M.; Manzoni, C.; Brida, D.; Tomasello, G.; Orlandi, G.; Kukura, P.; Mathies, R. A.; Garavelli, M.; Cerullo, G. Conical intersection dynamics of the primary photoisomerization event in vision. *Nature* **2010**, *467*, 440–443.

(3) Nasu, K., Ed. *Photoinduced Phase Transitions*; World Scientific: Singapore, 2004.

(4) Halcrow, M. A., Ed. *Spin-Crossover Materials: Properties and Applications*; John Wiley & Sons: Chichester, U.K., 2013.

(5) Decurtins, S.; Gütlich, P.; Köhler, C. P.; Spiering, H.; Hauser, A. Light-induced excited spin state trapping in a transition-metal complex: The hexa-1-propyltetrazole-iron (II) tetrafluoroborate spin-crossover system. *Chem. Phys. Lett.* **1984**, *105*, 1–4.

(6) Marchivie, M.; Guionneau, P.; Howard, J. A. K.; Chastanet, G.; Létard, J. F.; Goeta, A. E.; Chasseau, D. Structural characterization of a photoinduced molecular switch. *J. Am. Chem. Soc.* **2002**, *124*, 194–195.

(7) Collet, E.; Watanabe, H.; Bréfuel, N.; Palatinus, L.; Roudaut, F.; Toupet, L.; Tanaka, K.; Tuchagues, J. P.; Fertey, P.; Ravy, S.; Toudic, B.; Cailleau, H. Aperiodic spin state ordering of bistable molecules and its photoinduced erasing. *Phys. Rev. Lett.* **2012**, *109*, No. 257206.

(8) Buron-Le Cointe, M.; Hébert, J.; Baldé, C.; Moisan, N.; Toupet, L.; Guionneau, P.; Létard, J. F.; Freysz, E.; Cailleau, H.; Collet, E. Intermolecular control of thermoswitching and photoswitching phenomena in two spin-crossover polymorphs. *Phys. Rev. B* **2012**, *85*, No. 064114.

(9) Cobo, S.; Ostrovskii, D.; Bonhommeau, S.; Vendier, L.; Molnar, G.; Salmon, L.; Tanaka, K.; Bousseksou, A. Single-laser-shot-induced complete bidirectional spin transition at room temperature in single crystals of $(Fe^{II}(pyrazine)(Pt(CN)_4))$. *J. Am. Chem. Soc.* **2008**, *130*, 9019–9024.

(10) Lorenc, M.; Hébert, J.; Moisan, N.; Trzop, E.; Servol, M.; Buron-Le Cointe, M.; Cailleau, H.; Boillot, M. L.; Pontecorvo, E.; Wulff, M.; Koshihara, S.; Collet, E. Successive dynamical steps of photoinduced switching of a molecular Fe(III) spin-crossover material by time-resolved X-ray diffraction. *Phys. Rev. Lett.* **2009**, *103*, No. 028301.

(11) Bertoni, R.; Lorenc, M.; Tissot, A.; Boillot, M. L.; Collet, E. Femtosecond photoswitching dynamics and microsecond thermal conversion driven by laser heating in FeIII spin-crossover solids. *Coord. Chem. Rev.* **2015**, *282–283*, 66–76.

(12) Smeigh, A. L.; Creelman, M.; Mathies, R. A.; McCusker, J. K. Femtosecond time-resolved optical and Raman spectroscopy of photoinduced spin crossover: Temporal resolution of low-to-high spin optical switching. *J. Am. Chem. Soc.* **2008**, *130*, 14105–14107.

(13) Cannizzo, A.; Milne, C. J.; Consani, C.; Gawelda, W.; Bressler, C.; van Mourik, F.; Chergui, M. Light-induced spin crossover in Fe(II)-based complexes: The full photocycle unraveled by ultrafast optical and X-ray spectroscopies. *Coord. Chem. Rev.* **2010**, *254*, 2677–2686.

(14) McGarvey, J. J.; Lawthers, I.; Heremans, K.; Toftlund, H. Spin-state relaxation dynamics in iron(II) complexes: solvent on the activation and reaction and volumes for the $^1A$ $^5T$ interconversion. *J. Chem. Soc., Chem. Commun.* **1984**, 1575–1576.

(15) Khalil, M.; Marcus, M. M.; Smeigh, A. L.; McCusker, J. K.; Chong, H. H. W.; Schoenlein, R. W. Picosecond X-ray absorption spectroscopy of a photoinduced iron(II) spin crossover reaction in solution. *J. Phys. Chem. A* **2006**, *110*, 38–44.

(16) Wolf, M. M. N.; Groß, R.; Schumann, C.; Wolny, J. A.; Schünemann, V.; Døssing, A.; Paulsen, H.; McGarvey, J. J.; Diller, R. Sub-picosecond time resolved infrared spectroscopy of high-spin state formation in Fe(II) spin crossover complexes. *Phys. Chem. Chem. Phys.* **2008**, *10*, 4264–4273.

(17) Gawelda, W.; Cannizzo, A.; Pham, V. T.; van Mourik, F.; Bressler, C.; Chergui, M. Ultrafast nonadiabatic dynamics of $[FeII(bpy)_3]^{2+}$ in Solution. *J. Am. Chem. Soc.* **2007**, *129*, 8199–8206.

(18) Brady, C.; Toftlund, H.; McGarvey, J. J.; McCusker, J. K.; Hendrickson, D. N. In *Spin Crossover in Transition Metal Compounds III*, Gütlich, P., Goodwin, H.A., Eds.; Topics in Current Chemistry, Vol. 235; Springer: Berlin, 2004; p 1.

(19) Consani, C.; Prémont-Schwarz, M.; Elnahhas, A.; Bressler, C.; van Mourik, F.; Cannizzo, A.; Chergui, M. Vibrational coherences and

relaxation in the high-spin state of aqueous [Fe$^{II}$(bpy)$_3$]$^{2+}$. *Angew. Chem., Int. Ed.* 2009, *48*, 7184−7187.

(20) Huse, N.; Cho, H.; Hong, K.; Jamula, L.; de Groot, F. M. F.; Kim, T. K.; McCusker, J. K.; Schoenlein, R. W. Femtosecond soft X-ray spectroscopy of solvated transition-metal complexes: Deciphering the interplay of electronic and structural dynamics. *J. Phys. Chem. Lett.* 2011, *2*, 880−884.

(21) Lemke, H. T.; Bressler, C.; Chen, L. X.; Fritz, D. M.; Gaffney, K. J.; Galler, A.; Gawelda, W.; Haldrup, K.; Hartsock, R. W.; Ihee, H.; Kim, J.; Kim, K. H.; Lee, J. H.; Nielsen, M. M.; Stickrath, A. B.; Zhang, W.; Zhu, D.; Cammarata, M. Femtosecond X-ray absorption spectroscopy at a hard X-ray free electron laser: Application to spin crossover dynamics. *J. Phys. Chem. A* 2013, *117*, 735−740.

(22) Bressler, C.; Milne, C.; Pham, V. T.; El Nahhas, A.; van der Veen, R. M.; Gawelda, W.; Johnson, S.; Beaud, P.; Grolimund, D.; Kaiser, M.; Borca, C.; Ingold, G.; Abela, R.; Chergui, M. Femtosecond XANES study of the light-induced spin crossover dynamics in an iron(II) complex. *Science* 2009, *323*, 489−492.

(23) Juban, E. A.; Smeigh, A. L.; Monat, J. E.; McCusker, J. K. Ultrafast dynamics of ligand-field excited states. *Coord. Chem. Rev.* 2006, *250*, 1783−1791.

(24) Huse, N.; Kim, T. K.; Jamula, L.; McCusker, J. K.; de Groot, F. M. F.; Schoenlein, R. W. Photo-induced spin-state conversion in solvated transition metal complexes probed via time-resolved soft X-ray spectroscopy. *J. Am. Chem. Soc.* 2010, *132*, 6809−6816.

(25) Chergui, M. In *Spin-Crossover Materials*; Halcrow, M. A., Ed.; Wiley: West Sussex; 2013, pp 405−489.

(26) Bertoni, R.; Lorenc, M.; Tissot, A.; Servol, M.; Boillot, M. L.; Collet, E. Femtosecond spin-state photoswitching of molecular nanocrystals evidenced by optical spectroscopy. *Angew. Chem., Int. Ed.* 2012, *51*, 7485−7489.

(27) Lorenc, M.; Balde, C.; Kaszub, W.; Tissot, A.; Moisan, N.; Servol, M.; Buron-Le Cointe, M.; Cailleau, H.; Chasle, P.; Czarnecki, P.; Boillot, M. L.; Collet, E. Cascading photoinduced, elastic, and thermal switching of spin states triggered by a femtosecond laser pulse in an Fe(III) molecular crystal. *Phys. Rev. B* 2012, *85*, No. 054302.

(28) Collet, E.; Lorenc, M.; Cammarata, M.; Guérin, L.; Servol, M.; Tissot, A.; Boillot, M. L.; Cailleau, H.; Buron, M. L. 100 ps diffraction catches structural transients of laser-pulse triggered switching in a spin-crossover crystal. *Chem.—Eur. J.* 2012, *18*, 2051−2055.

(29) Collet, E.; Moisan, N.; Baldé, C.; Bertoni, R.; Trzop, E.; Laulhé, C.; Lorenc, M.; Servol, M.; Cailleau, H.; Tissot, A.; Boillot, M. L.; Graber, T.; Henning, R.; Coppens, P.; Buron, M. Ultrafast spin-state photoswitching in a crystal and slower consecutive processes investigated by femtosecond optical spectroscopy and picosecond X-ray diffraction. *Phys. Chem. Chem. Phys.* 2012, *14*, 6192−6199.

(30) Collet, E.; Boillot, M. L.; Hebert, J.; Moisan, N.; Servol, M.; Lorenc, M.; Toupet, L.; Buron-Le Cointe, M.; Tissot, A.; Sainton, J. Polymorphism in the spin-crossover ferric complexes [(TPA)-Fe$^{III}$(TCC)]PF$_6$. *Acta Crystallogr.* 2009, *B65*, 474−480.

(31) Marino, A.; Servol, M.; Bertoni, R.; Lorenc, M.; Mauriac, C.; Létard, J. F.; Collet, E. Femtosecond optical pump−probe reflectivity studies of spin-state photo-switching in the spin-crossover molecular crystals [Fe(PM-AzA)$_2$(NCS)$_2$]. *Polyhedron* 2013, *66*, 123−128.

(32) Marino, A.; Chakraborty, P.; Servol, M.; Lorenc, M.; Collet, E.; Hauser, A. The role of ligand-field states in the ultrafast photophysical cycle of the prototypical iron(II) spin-crossover compound [Fe-(ptz)$_6$](BF$_4$)$_2$. *Angew. Chem., Int. Ed.* 2014, *53*, 3863−3867.

(33) Cammarata, M.; Bertoni, R.; Lorenc, M.; Cailleau, H.; Di Matteo, S.; Mauriac, C.; Létard, J. F.; Matar, S.; Lemke, H.; Chollet, M.; Ravy, S.; Laulhé, C.; Collet, E. Sequential activation of molecular breathing and bending during spin-crossover photoswitching revealed by femtosecond optical and X-ray absorption spectroscopy. *Phys. Rev. Lett.* 2014, *113*, No. 227402.

(34) König, E.; Madeja, K. $^5T_2$ $^1A_1$ equilibria in some iron(II)-bis(1,l-phenanthroline) complexes. *Inorg. Chem.* 1967, *6*, 48−55.

(35) Müller, E. W.; Spiering, H.; Gütlich, P. Spin transition in [Fe(phen)2(NCS)2] and [Fe(bipy)2(NCS)2]: Hysteresis and effect of crystal quality. *Chem. Phys. Lett.* 1982, *93*, 567−571.

(36) Briois, V.; Cartier dit Moulin, Ch.; Sainctavit, Ph.; Brouder, Ch.; Flank, A. M. Full multiple scattering and crystal field multiplet calculations performed on the spin transition Fen(phen)$_2$(NCS)$_2$ Complex at the Iron K and L2,3 X-ray absorption edges. *J. Am. Chem. Soc.* 1995, *117*, 1019−1026.

(37) Baldé, C.; Desplanches, C.; Wattiaux, A.; Guionneau, P.; Gütlich, P.; Létard, J. F. Effect of metal dilution on the light-induced spin transition in [FexZn$_{1−x}$(phen)$_2$(NCS)$_2$] (phen = 1,10-phenanthroline). *Dalton Trans.* 2008, 2702−2707.

(38) Létard, J. F.; Guionneau, P.; Nguyen, O.; Costa, J. S.; Marcen, S.; Chastanet, G.; Marchivie, M.; Goux-Capes, L. A guideline to the design of molecular-based materials with long-lived photomagnetic lifetimes. *Chem.—Eur. J.* 2005, *11*, 4582−4589.

(39) Hohenberg, P.; Kohn, W. Inhomogeneous electron gas. *Phys. Rev. B* 1964, *136*, 864−871.

(40) Kohn, W.; Sham, L. J. Self-consistent equations including exchange and correlation effects. *Phys. Rev. A* 1965, *140*, 1133−1138.

(41) Frisch, M. J.; Trucks, G. W.; Schlegel, H. B.; Scuseria, G. E.; Robb, M. A.; Cheeseman, J. R.; Scalmani, G.; Barone, V.; Mennucci, B.; Petersson, G. A.; Nakatsuji, H.; Caricato, M.; Li, X.; Hratchian, H. P.; Izmaylov, A. F.; Bloino, J.; Zheng, G.; Sonnenberg, J. L.; Hada, M.; Ehara, M.; Toyota, K.; Fukuda, R.; Hasegawa, J.; Ishida, M.; Nakajima, T.; Honda, Y.; Kitao, O.; Nakai, H.; Vreven, T.; Montgomery, J. A., Jr.; Peralta, J. E.; Ogliaro, F.; Bearpark, M.; Heyd, J. J.; Brothers, E.; Kudin, K. N.; Staroverov, V. N.; Kobayashi, R.; Normand, J.; Raghavachari, K.; Rendell, A.; Burant, J. C.; Iyengar, S. S.; Tomasi, J.; Cossi, M.; Rega, N.; Millam, J. M.; Klene, M.; Knox, J. E.; Cross, J. B.; Bakken, V.; Adamo, C.; Jaramillo, J.; Gomperts, R.; Stratmann, R. E.; Yazyev, O.; Austin, A. J.; Cammi, R.; Pomelli, C.; Ochterski, J. W.; Martin, R. L.; Morokuma, K.; Zakrzewski, V. G.; Voth, G. A.; Salvador, P.; Dannenberg, J. J.; Dapprich, S.; Daniels, A. D.; Farkas, O.; Foresman, J. B.; Ortiz, J. V.; Cioslowski, J.; Fox, D. J. *Gaussian 09*, revision D.01; Gaussian, Inc.: Wallingford, CT, 2009.

(42) Zhang, W. K.; Alonso-Mori, R.; Bergmann, U.; Bressler, C.; Chollet, M.; Galler, A.; Gawelda, W.; Hadt, R. G.; Hartsock, R. W.; Kroll, T.; Kjar, K. S.; Kubicek, K.; Lemke, H. T.; Liang, H. W.; Meyer, D. A.; Nielsen, M. M.; Purser, C.; Robinson, J. S.; Solomon, E. I.; Sun, Z.; Sokaras, D.; van Driel, T. B.; Vanko, G.; Weng, T. C.; Zhu, D.; Gaffney, K. J. Tracking excited-state charge and spin dynamics in iron coordination complexes. *Nature* 2014, *509*, 345−348.

(43) van Veenendaal, M.; Chang, J.; Fedro, A. J. Model of ultrafast intersystem crossing in photoexcited transition-metal organic compounds. *Phys. Rev. Lett.* 2010, *104*, No. 067401.

(44) Chuang, J.; Fedro, A. J.; van Veenendaal, M. Ultrafast cascading theory of intersystem crossings in transition-metal complexes. *Phys. Rev. B* 2010, *82*, No. 075124.

(45) Baranovic, G.; Babic, D. Vibrational study of the Fe(phen)2-(NCS)2 spin-crossover complex by density-functional calculations. *Spectrochim. Acta A* 2004, *60*, 1013−1025.

(46) Ronayne, K. L.; Paulsen, H.; Höfer, A.; Dennis, A. C.; Wolny, J. A.; Chumakov, A. I.; Schünemann, V.; Winkler, H.; Spiering, H.; Bousseksou, A.; Gütlich, P.; Trautwein, A. X.; McGarvey, J. J. Vibrational spectrum of the spin crossover complex [Fe-(phen)$_2$(NCS)$_2$] studied by IR and Raman spectroscopy, nuclear inelastic scattering and DFT calculations. *Phys. Chem. Chem. Phys.* 2006, 4685−4693.

(47) Martin, R. Natural transition orbitals. *J. Chem. Phys.* 2003, *118*, 4775−4777.